Super-virtual Refraction Interferometry: Theory

Pawan Bharadwaj[1], *Gerard T. Schuster*[2] *and Ian Mallinson*[2]
[1] *King Abdullah University of Science and Technology and Indian School of Mines;* [2] *King Abdullah University of Science and Technology*

SUMMARY

Inverting for the subsurface velocity distribution by refraction traveltime tomography is a well-accepted imaging method by both the exploration and earthquake seismology communities. A significant drawback, however, is that the recorded traces become noisier with increasing offset from the source position, and so prevents accurate picking of traveltimes in far-offset traces. To enhance the signal-to-noise ratio of the far-offset traces, we present the theory of super-virtual refraction interferometry where the signal-to-noise ratio (SNR) of far-offset head-wave arrivals can be theoretically increased by a factor proportional to $\sqrt{N}$; here, N is the number of receiver and source positions associated with the recording and generation of the head-wave arrival. There are two steps to this methodology: correlation and summation of the data to generate traces with virtual head-wave arrivals, followed by the convolution of the data with the virtual traces to create traces with super-virtual head-wave arrivals. This method is valid for any medium that generates head-wave arrivals. There are at least three significant benefits to this methodology: 1). enhanced SNR of far-offset traces so the first-arrival traveltimes of the noisy far-offset traces can be more reliably picked to extend the useful aperture of data, 2). the SNR of head waves in a trace that arrive after the first arrival can be enhanced for accurate traveltime picking and subsequent inversion by traveltime tomography, and 3). common receiver-pair gathers can be analyzed to detect the presence of diving waves in the first arrivals, which can be used to assess the nature of the refracting boundary.

INTRODUCTION

Geophysicists have used wide-angle refraction surveys to image the gross crustal velocity structure of the earth (Funck et al., 2008; Zelt and Smith, 1992; Mooney and Weaver, 1989; Sheriff and Geldart, 1995), as well as the detailed structure within a few hundred meters of the near surface (Zhu et al., 1992). For wide-angle marine crustal studies, only a small number of Ocean Bottom Seismometers (OBS), often fewer than 100, are deployed while the source boat shoots at hundreds of shot points over a long range of offsets; the source-receiver offsets for OBS surveys can range from kilometers to tens of kilometers. Even fewer recording stations are sometimes deployed for a sonobuoy array.

A significant problem with current refraction surveys is that they require stronger sources in order to record first arrivals with high SNR at the far-offset traces. Without a sufficiently high SNR in the far-offset traces the refraction traveltimes cannot be accurately picked. To partly overcome this problem, Dong et al. (2006) presented the theory of refraction interferometry to increase the signal-to-noise ratio of head-wave arrivals. As illustrated in Figure 1a, the Dong et al. (2006) method windows about the head-wave arrivals and correlates a pair of traces to give $\phi(\mathbf{A},\mathbf{B})_x$, where **A** and **B** are the geophone positions; the resulting virtual trace contains a virtual refraction arrival with the arrival time of $\tau_{A'B} - \tau_{A'A}$. Repeating this procedure for any post-critical source position and the same geophone pair at **A** and **B** will lead to a virtual trace with the same refraction traveltime; hence, stacking over all post-critical source positions will yield a composite trace characterized by a virtual refraction event with an enhanced SNR. This enhancement can be as high as $\sqrt{N}$, where N is the number of sources that generates this particular head wave. They demonstrated this method on land field data shot over a salt dome in Utah, and later Nichols et al. (2010) demonstrated its effectiveness over a hydro geophysical research site in Idaho.

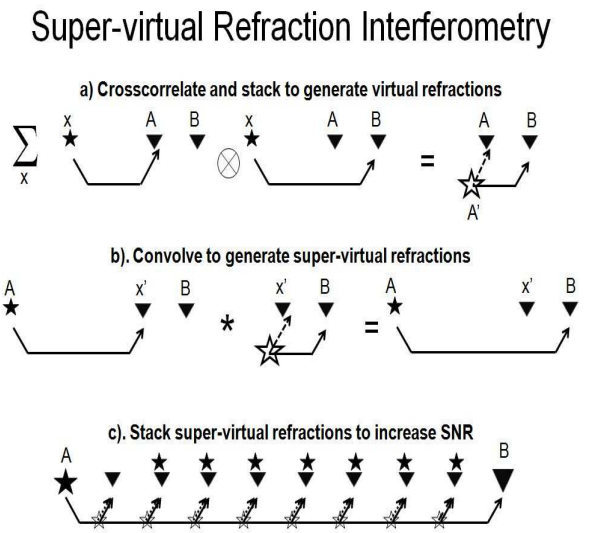

Figure 1: The steps for creating super-virtual refraction arrivals. a). Correlation of the recorded trace at **A** with that at **B** for a source at **x** to give the trace $\phi_x(\mathbf{A},\mathbf{B},t)$ with the virtual refraction having traveltime denoted by $\tau_{A'B} - \tau_{A'A}$. This arrival time will be the same for all post-critical source positions, so stacking $\sum_x \phi_x(\mathbf{A},\mathbf{B},t)$ will enhance the SNR of the virtual refraction by $\sqrt{N}$. b). Similar to that in a) except the virtual refraction traces are convolved with the actual refraction traces and stacked for different geophone positions to give the c). super-virtual trace with a SNR enhanced by $\sqrt{N}$. Solid (dashed) rays are associated with positive (negative) traveltimes.

A problem with refraction interferometry is that, if only the head-wave arrivals are correlated with one another, the virtual

head-wave trace has an unknown excitation time*, even though it has the correct moveout pattern. Another problem is that correlation of traces typically decreases the source-receiver offset of the virtual trace because traveltimes are subtracted and are associated with shorter raypaths (Schuster, 2009). To overcome these problems, Bharadwaj and Schuster (2010) and Mallinson et al. (2011) presented an extension of refraction interferometry so that the receiver spread could be extended to its maximum recording extent and the absolute arrival time is properly accounted for. This new method creates virtual far-offset refraction arrivals by a combination of both correlation and convolution of traces with one another (see Figure 1b) to create what is denoted as super-virtual refraction traces. Mallinson et al. (2011) presented the work flow of super-virtual refraction interferometry and demonstrated its effectiveness with both synthetic and field data results, but only gave an intuitive explanation of its underlying principles. In our new paper, we present the rigorous theory of super-virtual refraction interferometry.

The first part of this paper presents the theory of super-virtual refraction interferometry, and some synthetic examples are shown. The last section presents a summary.

THEORY

We will first present the far-field reciprocity equations of correlation and convolution types, and then show how they can be used to construct super-virtual refractions. The use of the the far-field reciprocity equation to create virtual refractions and enhance their SNR is a restatement of Dong et al. (2006), but convolving them with refraction data to create long-offset refraction traces is the key innovation in our paper. We will assume an acoustic medium with an arbitrary velocity distribution with constant density, and wide-band sources with unity amplitude at each frequency.

Reciprocity Equations of Correlation Type

Assume a source at $\mathbf{x}$ in Figures 1a and 2a and receivers at $\mathbf{A}$ and $\mathbf{B}$. The reciprocity theorem of correlation type (Wapenaar and Fokkema, 2006) states that the virtual Green's function $G(\mathbf{A}|\mathbf{B})^{virt\cdot}$ is given by the reciprocity theorem of correlation type:

$$\mathbf{B},\ \mathbf{A} \in V_0;\ \ 2iIm[G(\mathbf{A}|\mathbf{B})^{virt\cdot}] = \int_{top} [G(\mathbf{B}|\mathbf{x})^* \frac{\partial_x G(\mathbf{A}|\mathbf{x})}{\partial n} - G(\mathbf{A}|\mathbf{x}) \frac{\partial_x G^*(\mathbf{B}|\mathbf{x})}{\partial n}] d^2x, \quad (1)$$

where $\frac{\partial_x G(\mathbf{B}|\mathbf{x})}{\partial n} = \nabla G(\mathbf{B}|\mathbf{x}) \bullet \hat{n}$ for the outward point unit normal $\hat{n}$ on the boundary. Here, Green's function solves the Helmholtz equation for an arbitrary velocity distribution with a constant density (we follow the notation from Schuster (2009)). The integration path is only over the *top* path as the half-circle path is neglected by the Wapenaar anti-radiation condition.

To avoid artifacts due to a limited recording aperture and discrete sampling Dong et al. (2006) suggested windowing about the first arrivals so that only head wave arrivals are correlated with one another. In this case, $G(\mathbf{A}|\mathbf{B})$ is replaced by the head-wave arrival term defined as $\mathscr{G}(\mathbf{A}|\mathbf{B})$ to give, under the far-field approximation†,

$$Im[\mathscr{G}(\mathbf{A}|\mathbf{B})^{virt\cdot}] \approx k \int_{top} \mathscr{G}(\mathbf{A}|\mathbf{x})^* \mathscr{G}(\mathbf{B}|\mathbf{x}) d^2x, \quad (2)$$

where k is the average wavenumber and $\mathscr{G}(\mathbf{A}|\mathbf{B}) = G(\mathbf{A}|\mathbf{B})^{head}$ represents the head wave contribution in the Green's function for a specific interface. This approximation is analogous to that used in redatuming reflection data to a new datum where $\mathscr{G}(\mathbf{A}|\mathbf{x})^*$ is a model-based extrapolation Green's function that only accounts for direct arrivals, and $\mathscr{G}(\mathbf{x}|\mathbf{B})$ represents the reflection data devoid of direct waves and multiples.

According to the ray diagram in Figure1b, the correlated trace‡ $\mathscr{F}^{-1}(\mathscr{G}(\mathbf{A}|\mathbf{x})^* \mathscr{G}(\mathbf{B}|\mathbf{x}))$ for a source at $\mathbf{x}$ has the same kinematics as the correlated trace $\mathscr{F}^{-1}(\mathscr{G}(\mathbf{A}|\mathbf{x}')^* \mathscr{G}(\mathbf{B}|\mathbf{x}'))$ for a source§ at $\mathbf{x}'$. Such sources are considered to be at stationary points, and similar to surface wave interferometry (Xue et al., 2009), tend to enhance the SNR of the virtual head-wave arrival (Dong et al., 2006) by a factor of $\sqrt{N}$. Here, N represents the number of source positions that generate this type of head wave.

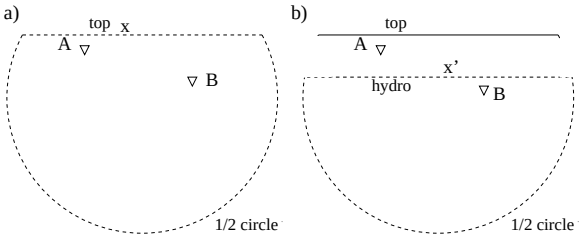

Figure 2: a). Geometry for computing virtual Green's functions $G(\mathbf{A}|\mathbf{B})$ from the recorded data $G(\mathbf{A}|\mathbf{x})$ and $G(\mathbf{B}|\mathbf{x})$ using the reciprocity theorem of correlation type in an arbitrary acoustic medium of constant density. b). Geometry for computing super-virtual Green's functions $G(\mathbf{B}|\mathbf{A})^{super}$ from the recorded data $G(\mathbf{A}|\mathbf{x}')$ and the virtual data $G(\mathbf{B}|\mathbf{x}')^{virt\cdot}$ using the reciprocity theorem of convolution type.

Reciprocity Equations of Convolution Type

It is assumed that the virtual data $G(\mathbf{B}|\mathbf{A})^{virt\cdot}$ can be extrapolated to get $G(\mathbf{x}'|\mathbf{A})^{virt\cdot}$ for $\mathbf{x}'$ along the horizontal dashed line in Figure 1b; similarly, the field data can be extrapolated to get $G(\mathbf{x}'|\mathbf{B})$. In this case, the reciprocity theorem of convolution type (Schuster, 2009) can then be employed:

$$G(\mathbf{B}|\mathbf{A}) = \int_{hydro} [G(\mathbf{B}|\mathbf{x}') \frac{\partial_{\mathbf{x}'} \mathbf{G}(\mathbf{A}|\mathbf{x}')}{\partial \mathbf{n}} - \mathbf{G}(\mathbf{A}|\mathbf{x}') \frac{\partial_{\mathbf{x}'} \mathbf{G}(\mathbf{B}|\mathbf{x}')}{\partial \mathbf{n}}] \mathbf{d^2 x}', \quad (3)$$

*It was suggested in Dong et al. (2006) that the source can be "virtually" relocated to the surface by calibrating the virtual stacked refraction trace to an observed traveltime in the raw data.

†For a marine survey, the $G(\mathbf{A}|\mathbf{x})$ can be recorded by towed hydrophones (or ocean bottom seismometers) positioned beneath the sources at $\mathbf{x}\varepsilon$ *top*. To satisfy the far-field approximation, it is assumed that the down going ghosts from the free surface have largely been removed. We have implicitly assumed that the source wavelet amplitude is zero phase and has the amplitude value of 1. More generally, the wavelet power spectrum can be included to take into account source wavelet effects.

‡$\mathscr{F}^{-1}$ denotes the temporal inverse Fourier transform.

§This assumes that the two sources are beyond the critical offset and the head waves emerge from the same refracting boundary.

where the integration is along the *hydro* dashed line in Figure 2b and the integration along the half-circle is negligible by the Sommerfeld radiation condition. Assuming the far-field approximation and setting $G \rightarrow \mathscr{G}$ yields the expression for the trace with the super-virtual head wave:

$$\mathscr{G}(\mathbf{B}|\mathbf{A})^{super} \approx 2ik \int_{hydro} \mathscr{G}(\mathbf{B}|\mathbf{x}')^{virt.} \mathscr{G}(\mathbf{A}|\mathbf{x}') d^2x', \quad (4)$$

where $\mathscr{F}^{-1}[\mathscr{G}(\mathbf{B}|\mathbf{A})^{super}]$ is the super-virtual trace obtained by convolving the recorded data $\mathscr{F}^{-1}[\mathscr{G}(\mathbf{A}|\mathbf{x}')]$ with the virtual data $\mathscr{F}^{-1}[\mathscr{G}(\mathbf{B}|\mathbf{x}')^{virt.}]$. Compared to the raw trace, the super-virtual head-wave arrival has a SNR enhanced by the factor $\sqrt{N}$, which means the combined enhancement using both equations 2 and 4 can be as high as N if the virtual data are convolved with the super-virtual data! However, practical considerations such as artifacts associated with limited recording apertures, discrete source and receiver sampling, windowing of the head waves, and the far-field approximation will likely prevent the attainment of this ideal enhancement.

In the synthetic section, we will use the example of head waves that have been windowed from the original data so that $G(\mathbf{x}|\mathbf{y}) \approx G(\mathbf{x}|\mathbf{y})^{head}$, but it will be understood that this procedure is valid for diving waves as well if the time window is opened up to include all arrivals. A desirable property of head waves, similar to that of surface waves (Xue et al., 2009), is that almost every surface source position in the post-critical region is a stationary point for a fixed pair of in-line receivers and a 2D medium; hence, a virtual head wave is reinforced at almost every inline source position for the specified receiver pair. This is not true if the refraction arrival is a pure diving wave, so the SNR of virtual diving waves will not be greatly increased.

SYNTHETIC DATA EXAMPLE

Synthetic common shot gathers are generated by a finite-difference solution to the 2D acoustic wave equation for the velocity model shown in Figure 3. A typical common receiver pair gather (CPG) and a shot gather are shown in Figure 4, with the geophone pair distance equal to 1500 m.

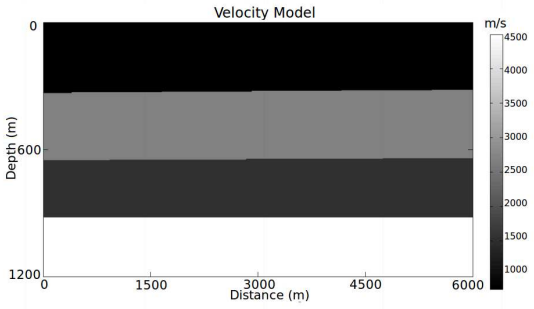

Figure 3: Acoustic velocity model used for generating the synthetic CSG in Figure 4b. The source and recording lines are 15 meters beneath the free surface and the source wavelet is a Ricker wavelet with a peak frequency of 15 Hz. The 59 sources and 250 receivers are spaced at 15 m intervals.

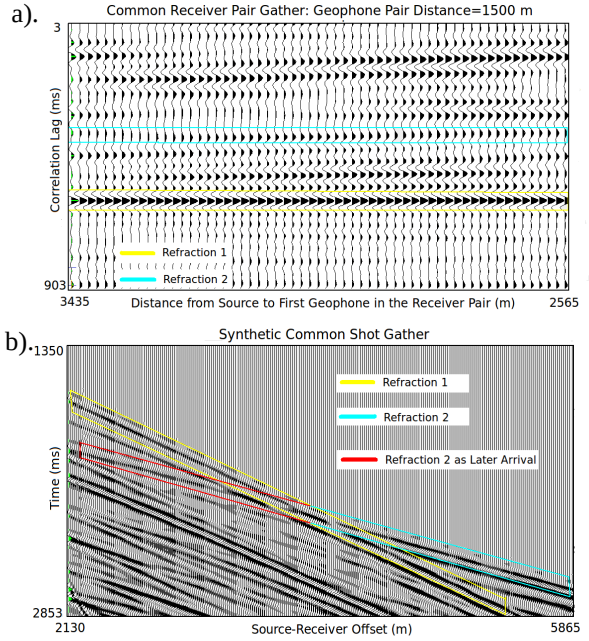

Figure 4: a). CPG (Dong et al., 2006) where the receivers are separated by 1500 m. Horizontal events in this gather will represent head-wave refractions even if the refracting boundary is irregular. b). A synthetic CSG with a surface source located 165 m from the upper left corner of the Figure 3 velocity model. First arrivals (yellow and blue lines) and later refraction arrivals before the cross-over offset (red lines) are highlighted.

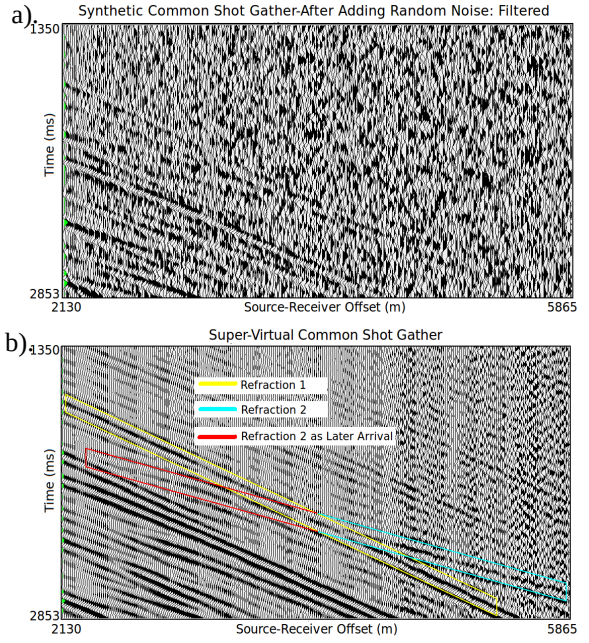

Figure 5: a) Figure 4b synthetic shot gather after addition of white noise. b) Super-virtual CSG with an improved SNR. Traveltime picking of first arrivals (blue and yellow lines) and later refraction arrivals (red lines) are greatly enhanced.

Random noise is now added to all the synthetic CSGs (an example is in Figure 5a) to test the sensitivity of the method to additive noise. The noisy CSGs show that the SNR of the far-offset traces is as low as 0.2 so that the first arrivals cannot be picked even after band-pass filtering. To remedy this problem, the traces are correlated and summed (see equation 2) to create virtual traces; and then convolving these virtual traces (after dip filtering to eliminate coherent noise) with the raw traces yields, after stacking (see equation 4), the super-virtual traces shown in Figure 5b; these traces were also dip filtered to eliminate coherent artifacts[¶]. It is obvious that most of the first arrival traveltimes can be now be picked in the super-virtual traces compared to the raw traces in Figure 5a. Even refraction arrivals that arrive after the first arrival can be identified in the red box shown in Figure 5b.

To validate the accuracy of the picked traveltimes, first arrival times are picked in the super-virtual shot gather and Figure 6a compares them to the traveltimes picked from the raw data. The difference in the these traveltimes is mostly within $T/4 = 0.017\ s$ of each other as shown in Figure 6b. This is consistent with the field data results of Mallinson et al. (2011) where more than 90 percent of the picked traveltimes agreed within a quarter of a period of the actual traveltimes for the raw traces with pickable events.

The super-virtual traces are obtained by the correlation and convolution of the raw traces so that the super-virtual source wavelet becomes ringy. This can lead to an ambiguous identification of the first arrival, so that there might be a discrepancy in the picked virtual traveltime with respect to the actual arrival time. This discrepancy can be identified by comparing the super-virtual traveltime to the actual traveltime picked from a trace with a high SNR. Alternatively, the super-virtual traces can be deconvolved by the autocorrelation of the wavelet prior to picking.

CONCLUSIONS

We presented the general theory of super-virtual refraction interferometry where the signal-to-noise ratio (SNR) of far-offset head-wave arrivals can be theoretically increased by a factor proportional to $\sqrt{N}$; here, N is the number of coincident receiver and source positions at post-critical offset. There are two steps to this methodology: correlation and summation of the data to generate traces with virtual head-wave arrivals, followed by the convolution of the data with the virtual traces to create traces with super-virtual head-wave arrivals. This method is valid for any medium that generates head-wave arrivals at the geophones. There are at least three significant benefits to this methodology: 1). enhanced SNR of far-offset traces so the first-arrival traveltimes of the noisy far-offset traces can be more reliably picked to extend the useful aperture of data, 2). the SNR of head waves that arrive later than the first

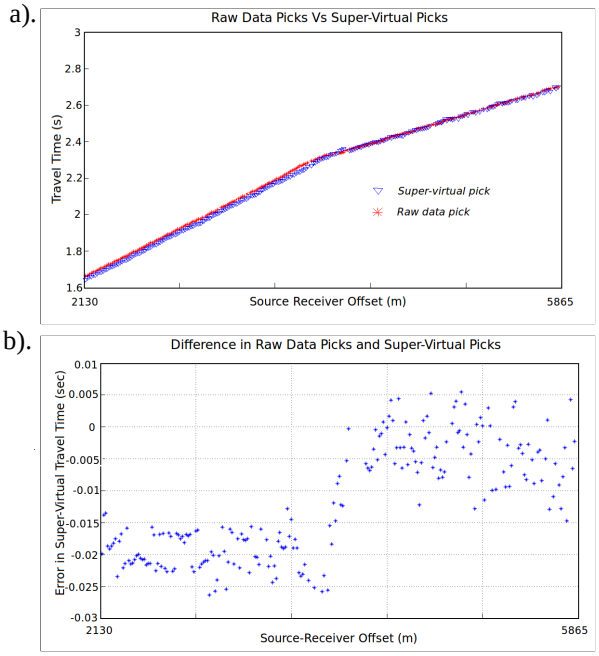

Figure 6: Plots showing a).picked traveltimes for the raw traces and super-virtual traces for a synthetic common shot gather and b). their difference in travel time picks.

arrival can be enhanced for accurate traveltime picking and subsequent inversion by traveltime tomography (Mallinson et al., 2011), and 3). common receiver-pair gathers (Dong et al., 2006) can be analyzed to detect the presence of diving waves in the first arrivals, which can be used to assess the nature of the refracting boundary.

The problems with this method are twofold. First, there will be artifacts in the super-virtual traces for a limited recording aperture and a coarse spacing of the source and receivers. This will lead to destructive interference with the super-virtual events. Partial remedies might be dip filtering, windowing, or least-squares redatuming (Xue, 2009; Wapenaar et al., 2008). Secondly, if the refraction arrivals are primarily diving waves, then, unlike head waves, there are not so many stationary source positions on the surface for a fixed pair of receivers. Hence, the SNR of virtual diving waves will not be greatly increased by this algorithm.

[¶]There are three different processing procedures that might be used to compute super-virtual events with high quality. Procedure 1 is to correlate and stack the raw records to create virtual traces, then convolve these virtual traces with the raw traces and sum over appropriate receiver positions. Procedure 2 is the same as procedure 1 except the raw traces and virtual traces are windowed about the expected first arrivals. Procedure 3 is the same as 1 or 2 except dip filters are used to eliminate unwanted dipping events in both the raw data and virtual data. The traces at and near the shot location should be muted.

EDITED REFERENCES

Note: This reference list is a copy-edited version of the reference list submitted by the author. Reference lists for the 2011 SEG Technical Program Expanded Abstracts have been copy edited so that references provided with the online metadata for each paper will achieve a high degree of linking to cited sources that appear on the Web.

REFERENCES

Bharadwaj, P., and G. T. Schuster, 2010, Extending the aperture and increasing the signal-to-noise ratio of refraction surveys with super-virtual interferometry: AGU Annual Meeting Abstracts.

Dong, S., J. Sheng, and G. T. Schuster, 2006, Theory and practice of refraction interferometry: 76th Annual International Meeting, SEG, Expanded Abstracts, **25**, 3021–3025.

Funck, T., M. Anderson, and J. Neish, 2008, A refraction seismic transect from the Faroe islands to the Hatton-Rockall basin: Journal of Geophysical Research, **113**, B12, B12405, doi:10.1029/2008JB005675.

Mallinson, I., P. Bharadwaj, G. T. Schuster, and H. Jakubowicz, 2011, Enhanced refractor imaging by super-virtual inteferometry: The Leading Edge, **30**, 546–550.

Mooney, W. D., and C. S. Weaver, 1989, Regional crustal structure and tectonics of the pacific coastal states: California, Oregon, and Washington: Geophysical framework of the continental United States: Geological Society of America Memoir, 172, 129–161.

Nichols, J., D. Mikesell, and K. V. Wijk, 2010, Application of the virtual refraction to near-surface characterization at the Boise hydrogeophysical research site: Geophysical Prospecting, **58**, 1011–1022.

Schuster, G. T., 2009, Seismic interferometry: Cambridge University Press.

Sheriff, R., and L. Geldart, 1995, Exploration seismology: Cambridge University Press.

Wapenaar, K., and J. Fokkema, 2006, Green's function representations for seismic interferometry: Geophysics, **71**, no. 4, SI33–SI46, doi:10.1190/1.2213955.

Wapenaar, K., J. van der Neut, and E. Ruigrok, 2008, Passive seismic interferometry by multidimensional deconvolution: Geophysics, **73**, no. 6, A51–A56, doi:10.1190/1.2976118.

Xue, Y., 2009, Least-squares datuming and surface waves prediction with interferometry: PhD thesis, University of Utah.

Xue, Y., S. Dong, and G. T. Schuster, 2009, Interferometric prediction and subtraction of surface waves with a nonlinear local filter: Geophysics, **74**, no. 1, SI1–SI8, doi:10.1190/1.3008543.

Zelt, C., and R. Smith, 1992, Seismic traveltime inversion for 2D crustal velocity structure: Geophysical Journal International, **108**, no. 1, 16–34, doi:10.1111/j.1365-246X.1992.tb00836.x.

Zhu, X., D. P. Sixta, and B. G. Angstman, 1992, Tomostatics: Turning-ray tomography + static corrections: The Leading Edge, **11**, 15–23, doi:10.1190/1.1436864.